

Primary Extragenadal Yolk Sac Tumor Arising from the Urachus: A Case Report with Literature Review

Kenneth Steven Taylor^{1*}, Kristian Theo Schafernak¹, Lisa McMahon², David Notrica², Masayo Watanabe³, Carrie Schaefer⁴ and Paul Dickman¹

¹Department of Pathology and Laboratory Medicine, Phoenix Children's Hospital, 1919 E Thomas Rd, Phoenix, AZ, 85016

²Department of Surgery, Phoenix Children's Hospital, 1919 E Thomas Rd, Phoenix, AZ, 85016

³Center for Hematology and Oncology, Phoenix Children's Hospital, 1919 E Thomas Rd, Phoenix, AZ, 85016

⁴Department of Radiology, Phoenix Children's Hospital, 1919 E Thomas Rd, Phoenix, AZ, 85016

ABSTRACT

Germ cell tumors in extragenadal sites are uncommon; those arising in the urachus are exceedingly rare and limited to a few anecdotal reports. Herein we document an occurrence of yolk sac tumor in a 9-month-old male who presented with abdominal distension. Laboratory investigation revealed elevated lactate dehydrogenase and α -fetoprotein levels; imaging studies were inconclusive as to tumor type or site of origin. The tumor was resected from the base of the umbilicus and histologic examination revealed neoplastic cells arranged in solid nests or microcystic patterns in a fibromyxoid stroma. Schiller-Duval bodies were conspicuous. Immunohistochemical analysis showed lesional cells reactive to α -fetoprotein, SALL4, placental alkaline phosphatase, Glypican-3 and CD117. No teratomatous or other germ cell elements were identified. These findings supported a diagnosis of pure yolk sac tumor arising from the urachus; the clinical, radiological and pathological findings are discussed.

Keywords: *Urachus Extra-Gonadal Germ Cell Tumor Yolk Sac Tumor Immunohistochemistry Pediatric Pathology*

Introduction

The urachus is a vestigial structure, the fibrous remnant of the allantois, a canal that drains the fetal urinary bladder and joins the umbilical cord. It typically regresses following the fifth gestational month to form the medial umbilical ligament.^[1] Persistence of the urachus is well-documented as are the lesions associated with this structure: cysts, fistulae, sinuses, diverticula, and neoplasms.^[1] Although rare, adenocarcinoma is the most common urachal malignancy; extragenadal germ cell tumors (EGCT) arising in this location are exceptionally rare.^[1] Herein we report an EGCT in a 9-month-old male adding to the small number of documented reports of urachal yolk sac tumor (YST).^[1]

Case Report

The patient was a 9-month-old male who presented to his pediatrician for abdominal distention, abdominal wall venous engorgement and eversion of the umbilicus. An ultrasound (US) examination demonstrated the presence of an abdominal mass (8 cm) and the patient was referred to our institution for further evaluation. Initial laboratory investigation included a normal complete metabolic panel; lactate dehydrogenase (LDH) was elevated at 532 U/L (normal: 81-234 U/L). Computed-tomography (CT) with contrast of the abdomen and pelvis (**Figs.**

1A-C) demonstrated the presence of a heterogeneously enhancing mesenteric mass (9.0 x 8.7 x 7.2 cm). Areas of low density, reflecting necrosis or cystic change, were present. Enlarged vessels in the anterior abdominal wall extended into the anterior aspect of the mass. A large amount of free intraperitoneal fluid suggested ascites or tumor rupture. A follow-up abdominal US further delineated the presence of feeding arteries arising from the anterior abdominal wall extending into the anterior aspect of the mass (**Fig. 1D**). A host of clinical and radiological impressions were considered in the differential diagnosis including inflammatory pseudotumor, rhabdomyosarcoma, neuroblastoma, congenital hemangioma and teratoma.

The possibility of teratoma prompted additional testing to determine α -fetoprotein (AFP) and beta-human chorionic gonadotropin (β -hCG) concentrations. The β -hCG level was normal, but AFP was markedly elevated at 44,481 ng/mL (normal: 0-90 ng/mL). Subsequent blood examination revealed thrombocytopenia and platelets were administered. At laparoscopy, a moderate amount of remote hemorrhage was encountered and fluid was sent for cytologic interpretation. The mass displayed focal omental adhesions and appeared to originate from the anterior abdominal wall. A biopsy of the mass was sent for intraoperative analysis which revealed a high-grade tumor composed of mildly to moderately hypertrophic cells with

hyperchromatic, pleomorphic nuclei in a fibromyxoid stroma. The procedure was converted to an en-bloc removal and the extirpation emanated from the urachus.

The specimen consisted of a well-circumscribed tumor (11.2 x 8.7 x 7.2 cm) with urachal stump (**Fig. 2A**). Cut surfaces showed an encapsulated tan-gray to yellow, myxoid tumor with a vaguely nodular architecture admixed with scattered foci of hemorrhage and necrosis (**Fig. 2B**). The tumor was present at several margins, including several surface defects. Touch imprints of the resection were stained with Diff-Quik and hematoxylin and eosin (H&E) which were highly cellular with individual, clusters or sheets of cells with variable cytoplasm, with or without vacuoles. The nuclei were pleomorphic with vesicular chromatin, usually with one or more conspicuous nucleoli.

Multiple foci of metachromatic pink hyaline basement membrane-like material were present (**Fig. 3A**). Given these cytologic findings, the location of the mass, and an elevated AFP level, the possibility of yolk sac tumor (YST) was added to the differential diagnosis.

Permanent sections further supported the diagnosis of YST, with tumor cells organized into microcystic or nested solid patterns (**Fig. 3B**) with pathognomonic Schiller-Duval bodies (**Fig. 3C**). No heterologous tissues or other germ cell tumor elements were identified. The tumor cells were immunoreactive with AFP (**Fig. 3D**), SALL4, glypican-3, CD117 (solid areas) and placental alkaline phosphatase (PLAP), and negative for OCT-4 and CD30. The overall features were those of pure YST arising from the urachus. Pelvic fluid cytology was negative for malignancy.

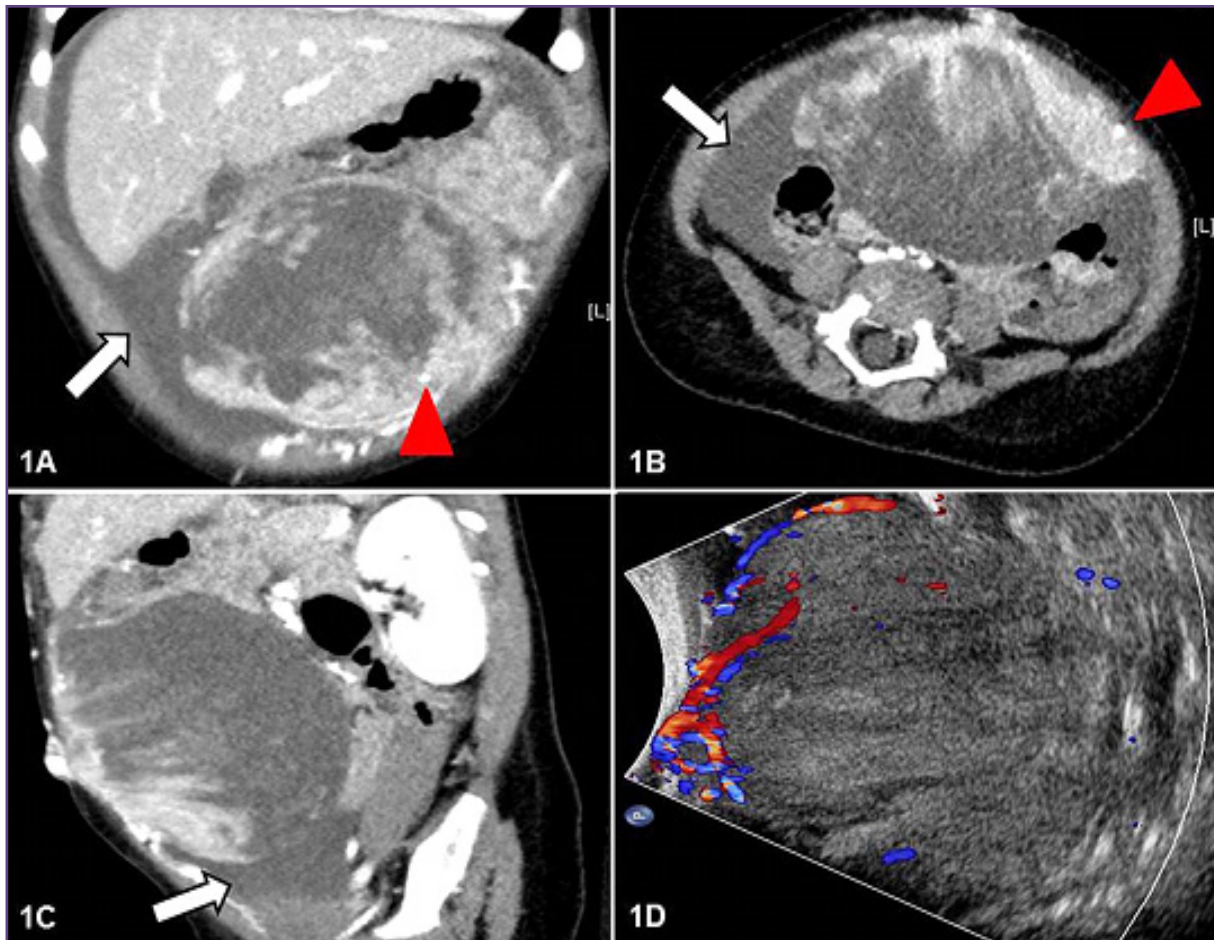


Fig. 1: Post-contrast CT imaging of the abdomen and pelvis in coronal (1A), axial (1B) and sagittal (1C) planes demonstrated the presence of a vascular heterogeneously enhancing mesenteric mass contiguous with the anterior abdominal wall. Free intraperitoneal fluid (arrow) is present as are prominent anterior abdominal wall vessels (wedge) permeating the anterior aspect of the mass (1A-C). A sagittal Doppler US image (1D) correlates well with the sagittal CT view (1C) and further delineates the vessels in the anterior abdominal wall which extend into the mass.

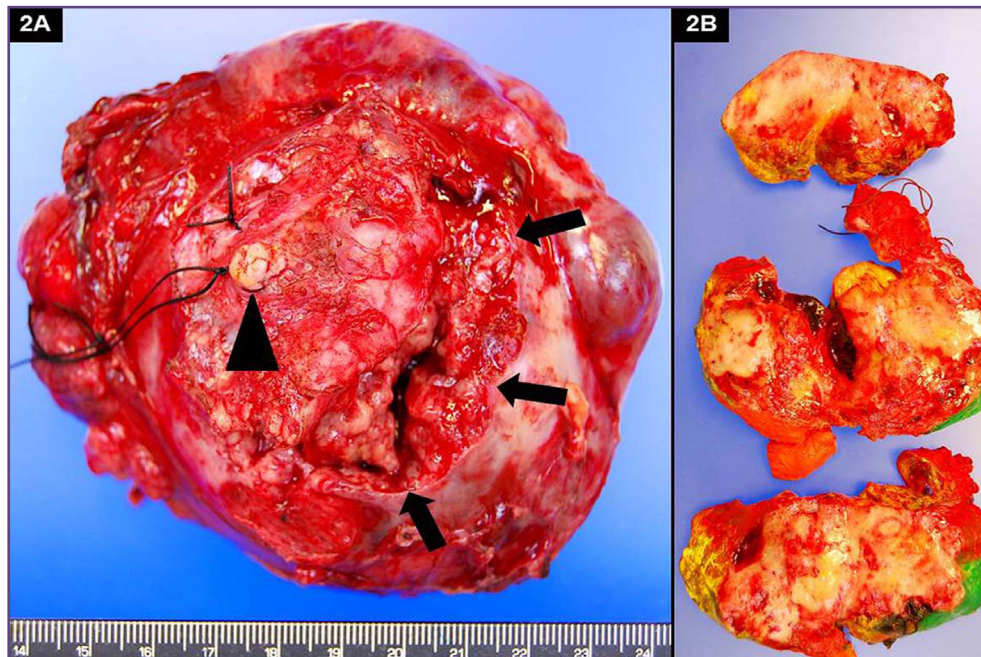


Fig. 2: Macroscopic view of the resected abdominal mass (2A) revealed a circumscribed tumor with several defects (arrows) and a stump of urachus (wedge). Cut surfaces (2B) demonstrated heterogeneous tan-gray, tan-yellow and red tissue with glistening cut surfaces admixed with foci of hemorrhage and necrosis. Note the extension of the mass to multiple resection margins and associated blood clot at disrupted areas.

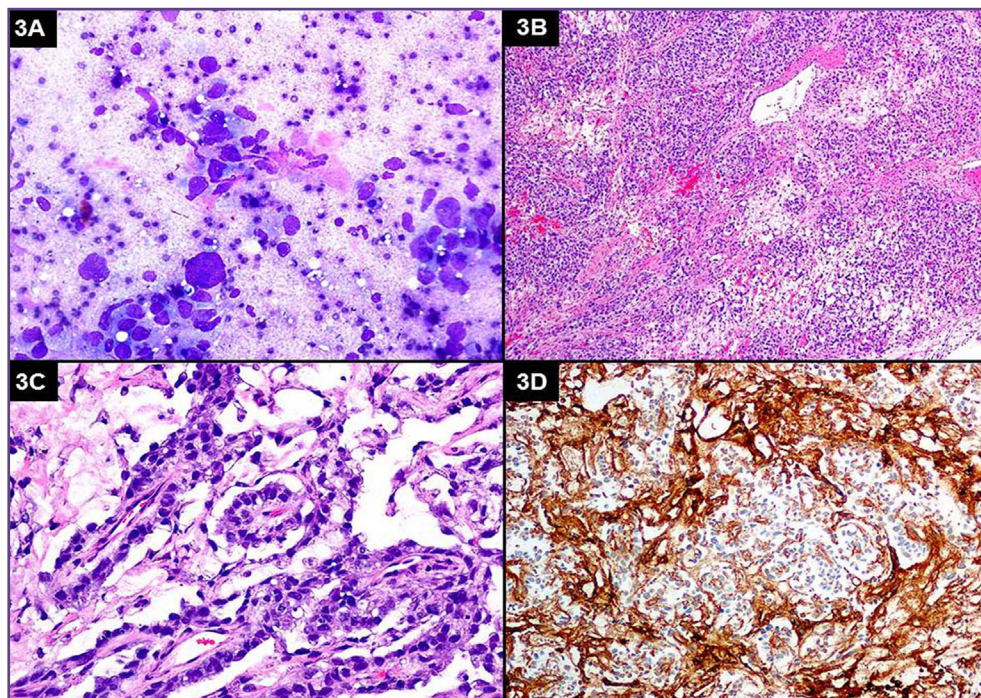


Fig. 3: Touch preparations (3A) from the resection specimen showed intermediate to large, pleomorphic, neoplastic cells with nuclear and cytoplasmic vacuoles. Note the central metachromatic, pink, hyaline basement membrane-like material (Diff-Quik x 200). Routine H&E stained preparations revealed lesional cells arranged in solid nests or microcystic patterns (3B x 40). Structures lined by festooning, pseudopapillary projections with a central vascular core were diagnostic of Schiller-Duval bodies (3C x 200) and lesional cells were immunohistochemically decorated with AFP (3D x 100).

Discussion

During embryologic development, the allantois and cloaca regress, leading to the formation of the urachus, which is anchored to the dome of the bladder and the umbilicus.^[1] Although infrequent, adenocarcinoma is the most common malignant neoplasm, representing 0.35-0.7% of the urinary bladder tumors.^[2] Even more rare are EGCTs arising in the urachus where, to our knowledge, only three previous cases of YST have been documented.^[1,3,4] Most germ cell tumors (GCT) occur in the gonads, but ~20% of cases arise in other locations: mediastinum, sacrococcygeal region, retroperitoneum, cervix, vulva, pelvis, lung, head/neck, stomach, omentum, bladder, endometrium, kidney, prostate and liver.^[5-10] Several hypotheses have been offered to explain the histogenesis of EGCTs and include (1) arrested migration or misplacement of germ cells during development, (2) reverse migration of germ cells, (3) aberrant differentiation of somatic cells, (4) derivation from pluripotent stem cells within a somatic tumor, (5) origination from residual fetal tissue following incomplete abortion (uterine-based lesions), and (6) metastases from an occult gonadal primary malignancy.^[11] Given the midline tumor location, the sex of the patient and the absence of either a testicular or other occult primary, we speculate that theories 1-3 are applicable; nevertheless, a definitive characterization is not possible. YSTs comprise approximately 20% of high-grade GCTs and are the most common malignant germ cell tumors in infants and children <4 years of age and represent 3-5% of pediatric tumors.^[12] YSTs grow rapidly and can metastasize via lymphatic or hematogenous routes.^[6] These tumors typically elaborate AFP, and, although detection of elevated AFP levels is sensitive, it is not specific. Other lesions, such as those included in the differential diagnosis of the present case (teratoma and rarely rhabdomyosarcoma), can also elaborate AFP.^[13,14]

The radiological features of YST are not specific; however, familiarity with its imaging characteristics can enable preoperative diagnosis, improve surgical planning and assess effects of treatment.^[15-19] The CT findings in two cohorts with a combined total of 31 YSTs (age range: 1-31 years) documented that lesions ranged from 5-24 cm and most were well-circumscribed with defined borders.^[15,16] Intralesional calcification was rare; however, intratumoral hemorrhage, ascites and marked enhancement were common findings.^[15,16] Further, enhancement of intratumoral vessels was detected in 90% of cases.^[15,16] These vessels typically contain a dilated lumen that on postcontrast imaging display a "bright dot" sign, considered a classical imaging feature of this entity.^[15] The enhancement is thought to result from increased vascularity, with the formation of small vascular

aneurysms within the tumor.^[15] As provided above, the CT findings in the present case were consistent with previously published results.

Cytological analysis is extremely useful in the diagnosis of malignant neoplasms and an accepted alternative to routine tissue diagnosis.^[20,21] Common cytological features of YSTs include highly cellular specimens in which neoplastic cells are arranged singly, in loosely cohesive clusters, in papillary or microglandular patterns.^[20-22] Tumor cells are intermediate to large with scant to moderate cytoplasm, typically with a high nuclear:cytoplasmic ratio.^[20,21] Neoplastic nuclei reveal irregular contours with at least one prominent nucleolus.^[20,21] Cytoplasmic and nuclear vacuoles, apoptotic bodies, mitotic figures, and background inflammatory infiltrates may be present in variable amounts.^[20,21] Characteristic Schiller-Duval bodies and periodic-acid Schiff (PAS) positive hyaline globules may also be present; however, these may be infrequent findings. In a study by Gupta *et al*, Schiller-Duval bodies were identified in only 10% of cytology cases while hyaline globules were present in 20%.^[21] An additional salient feature is the presence of hyaline basement membrane-like material, which metachromatically stains pink with Wright stains and green with Papanicolaou techniques.^[21] Exfoliative cytology in the present case demonstrated all of the above features save for Schiller-Duval bodies.

Grossly, YSTs are typically well-circumscribed tumors measuring up to 24 cm.^[15,16] These neoplasms are usually intact but have the potential to rupture as exemplified in the present case. Cut surfaces show grey tan to yellow, myxoid tissue admixed with hemorrhage and necrosis. Histologically, YSTs are high-grade neoplasms that can show myriad architectural patterns including reticular/microcystic, macrocystic, papillary, solid, parietal polyvesicular, sarcomatoid, glandular, hepatoid and Schiller-Duval bodies.^[8,12] This variability, in conjunction with extragonadal sites, can pose a diagnostic challenge. Identification of Schiller-Duval bodies is pathognomonic for YST; however, these structures are present in only 20% of tissue specimens.^[6] IHC plays a vital role in confirming the diagnosis of YST; however, a single, unique marker both sensitive and specific for this tumor is currently unavailable.^[8] Instead, a panel of IHC stains is necessary and should include a pluripotent germ cell marker (SALL4), antibodies associated with YST (AFP and glypican-3), and labels present in more differentiated yolk sac tumors (cytokeratin (CK) AE1/AE3, CK20, CDX2 and villin).^[8,11] In this case, lesional cells were moderately stained with AFP; strongly positive for SALL4, CK AE1/AE3, PLAP; and focally reactive for CD117. Tumor cells were negative for OCT-4 and CD30. Due to

its variety of histologic patterns, the differential diagnosis of extragonadal yolk sac tumors (EGYSTs) in pelvic or peritoneal locations include carcinomas primary to a specific site, such as clear cell carcinoma, endometrial cancer, or carcinosarcoma of the uterus, adnexal tissue or peritoneum; adenocarcinoma (with or without intestinal differentiation) of the urachus or bladder; and primary or metastatic gastrointestinal carcinoma.^[8] Each of these tumors is typically seen in adults; however, IHC can exclude these common neoplasms while assisting in the detection of a YST component.^[8] Most intra-abdominal GCTs result from metastatic disease, usually from a gonadal primary.^[23] Neither testicular nor mediastinal lesions were identified via imaging in the present case. Of the initial clinico-radiological considerations in this case, congenital hemangiomas possess a markedly different histoarchitecture and, further contrasting with YSTs, display positive expression of CD31, CD34 and Glut-1. Although neuroblastomas may harbor areas of hemorrhage and necrosis, these tumors usually contain calcifications, abundant neuropil, and demonstrate immunoreactivity with markers (NB84, CD56, synaptophysin) that are not associated with YSTs. Inflammatory pseudotumors are composed of ovoid to spindle cells without nuclear atypia or abnormal mitotic figures. The lesional cells are usually in a compact stroma admixed with a mixed inflammatory infiltrate. Although routine light microscopy easily distinguishes inflammatory pseudotumor from YST, immunohistochemistry may be used to exclude this diagnosis. With adequate sampling, heterologous elements seen in teratomas are easily recognized; however, no mature or immature features were present in this case. Rhabdomyosarcomas can display pleomorphic, bizarre nuclei, areas of hemorrhagic necrosis and mitotic activity. Further, the lesional cells in rhabdomyosarcoma are spindle-shaped with deeply eosinophilic cytoplasm and are immunoreactive for myogenin, MyoD1 and desmin.

Treatment of YST includes combination chemotherapy and surgical intervention; radiation is ineffective.^[5,6] Following clinical, radiological and pathological evaluations, parameters are used to determine the risk of disease and the management of previously untreated patients to determine the correct chemotherapeutic regimen.^[5] Patients are placed into low, intermediate or high risk categories based on anatomical location of the primary tumor, levels of biomarkers prior to beginning treatment, serum LDH values and overall tumor burden.^[5] The lesion in this case displayed several defects consistent with tumor rupture and the patient was assessed as intermediate risk with stage III disease. Chemotherapy typically consists of bleomycin, etoposide and cisplatin (BEP), which are

very effective; however, other agents (carboplatin) may be used.^[5,6] Adverse prognostic factors include age >11 years, extragonadal stage III or IV disease and high AFP levels.^[24] Of interest, two previously reported patients with urachal YST achieved complete remission following combination chemotherapy and surgery.^[1] Treatment efficacy is assessed by serial investigation of AFP levels, which can also alert clinical staff to disease recurrence. The patient in the case under review was treated according to the Children's Oncology Group AGCT01P1 protocol. Following four cycles of BEP, the patient's AFP levels have precipitously dropped from >44,000 to 13.8 U/mL. Radiological assessment can also be employed as a surveillance method and studies have demonstrated the utility of FDG-PET/CT not only in disease detection but also in assessing response to therapy.^[17-19] Of note, the role of novel biomarkers such as microRNAs (miR), which are short, non-protein-coding RNAs, has been investigated in disease states.^[25] MicroRNAs at a few 'clusters,' miR-371-373 and miR-302-367, are overexpressed in all malignant GCTs despite anatomical location, patient age or subtype.^[25] In the future, screening for these biomarkers may be useful in the diagnosis, surveillance and prognosis of GCTs.^[25]

Conclusion

Extragonadal germ cell tumors are uncommon and those arising in the urachus are exceedingly rare. Herein we discuss the findings of an extraordinary case of pure YST arising from the urachus. The variable sites of origin and infrequency of EGCTs can pose a diagnostic challenge. A midline tumor that elaborates elevated levels of AFP with imaging features associated with YST should prompt the clinical team to incorporate extragonadal yolk sac tumor in the differential diagnosis for rapid and accurate diagnosis.

Reference

1. Romero-Rojas AE, Messa-Botero OA, Melo-Urbe MA, Diaz-Perez JA, Chinchilla-Olaya SI. Primary yolk sac tumor of the urachus. *Int J Surg Pathol.* 2011; 19(5):658-661.
2. Sheldon CA, Clayman RV, Gonzalez R, Williams RD, Fraley EE. Malignant urachal lesions. *J Urol.* 1984; 131:1-8.
3. Huang HY, Ko SF, Chuang JH, Jeng YM, Sung MT, Chen WJ. Primary yolk sac tumor of the urachus. *Arch Pathol Lab Med.* 2002; 126:1106-1109.
4. D'Allesio A, Verdelli G, Bernardi M, et al. Endodermal sinus (yolk sac) tumor of the urachus. *Eur J Pediatric Surg.* 1994; 4(3):180-181.
5. Harano K, Ando M, Sasajima Y, et al. Primary yolk sac tumor of the omentum: a case report and literature review. *Case Rep Oncol.* 2012; 5:671-675.
6. Lim SH, Kim YH, Yim GW, et al. Primary omental yolk sac tumor. *Obstet Gynecol Sci.* 2013; 56(6):412-415.

7. Zeremski V, Mawrin C, Fischer T, Schalk E. Diagnostic and therapeutic challenges in extragonadal yolk sac tumor with hepatoid differentiation: a case report. *Mol Clin Oncol*. 2017; 6:79-82.
8. Ravishankar S, Malpica A, Ramalingam P, Euscher ED. Yolk sac tumor in extragonadal pelvic sites. Still a diagnostic challenge. *Am J Surg Pathol*. 2017; 41(1):1-11.
9. Joseph MG, Fellows FG, Hearn SA. Primary endodermal sinus tumor of the endometrium. A clinicopathologic, immunocytochemical, and ultrastructural study. *Cancer*. 1990; 65:297-302.
10. Lin SC, Li XH, Sun CH, et al. CT findings of intrarenal yolk sac tumor with tumor thrombus extending into the inferior vena cava: a case report. *Korean J Radiol*. 2014; 15(5):641-645.
11. Euscher ED. Unusual presentations of gynecologic tumors. Extragonadal yolk sac tumor of the vulva. *Arch Pathol Lab Med*. 2017; 141:293-297.
12. Arumugam D, Thandavarayan P, Chidambaram L, Boj S, Marudasalam S. Primary nasopharyngeal yolk sac tumor: a case report. *J Clin Diagn Res*. 2016; 10(5):ED06-ED07.
13. El-Bahrawy M. α -Fetoprotein-producing non-germ cell tumors of the urological system. *Rev Urol*. 2011;13(1):14-19.
14. Mori H, Matsubara N, Fujii M, et al. Alpha-fetoprotein producing rhabdomyosarcoma of the adult liver. *Pathol Int*. 1979;29(3):485-491.
15. Li YK, Zheng Y, Lin JB, et al. Radiological-pathological correlation of yolk sac tumor in 20 patients. *Acta Radiol*. 2016;57(1):98-106.
16. Li YK, Zheng, Lin JB, et al. CT imaging of ovarian yolk sac tumor with emphasis on differential diagnosis. *Sci Rep*. 2015; 5:11000; doi: 10.1038/srep11000.
17. Baba T, Su S, Umeoka S, et al. Advanced extragonadal yolk sac tumor serially followed up with 18F-fluorodeoxyglucose-positron emission tomography and computerized tomography and serum alpha-fetoprotein. *J Obstet Gynaecol Res*. 2012;38(3):605-609.
18. Takahashi M, Kanamori Y, Takahashi M, Momose T, Iwanaka T. Detection of a metastatic lesion and tiny yolk sac tumors in two teenage patients by FDG-PET: report of two cases. *Surg Today*. 2014;44:1962-1965.
19. Liu M, Chen G, Fu Z, Li Z, Li Q. Occult mediastinal yolk sac tumor producing α -fetoprotein detected by 18F-FDG-PET. *Clin Nuc Med*. 2016;41(7):585-586.
20. Gilbert KL, Bergman S, Dodd LG, Volmar KE, Creager AJ. Cytomorphology of yolk sac tumor of the liver in fine-needle aspiration: a pediatric case. *Diagn Cytopathol*. 2006;34(6):421-423.
21. Gupta R, Mathur SR, Arora VK, Sharma SG. Cytology features of extragonadal germ cell tumors. A study of 88 cases with aspiration cytology. *Cancer*. 2008;114(6):504-511.
22. Kataria SP, Misra K, Singh G, Kumar S. Cytological findings of an extragonadal yolk sac tumor presenting at an unusual site. *J Cytol*. 2015;32(1):62-64.
23. McKenney JK, Heerema-McKenney A, Rouse RV. Extragonadal germ cell tumors: a review with emphasis on pathologic features, clinical prognostic variables, and differential diagnostic considerations. *Adv Anat Pathol*. 2007;14(2):69-92.
24. Frazier AL, Hale JP, Rodriguez-Galindo C, et al. Revised risk classification for pediatric extracranial germ cell tumors based on 25 years of clinical trial data from the United Kingdom and United States. *J Clin Oncol*. 2015;33(2):195-201.
25. Murray MJ, Huddart RJ, Coleman N. The present and future of serum diagnostic tests for testicular germ cell tumors. *Nat Rev Urol*. 2016;13(12):715-725.

***Corresponding author:**

Kenneth Steven Taylor, Phoenix Children's Hospital, 1919 E Thomas Rd, Dpt. of Pathology and Laboratory Medicine, Phoenix, AZ 85016 USA

Phone: (602)-933-3036

Email: ktaylor3@phoenixchildrens.com

Financial or other Competing Interests: None.